Asian Journal of Chemistry; Vol. 25, No. 13 (2013), 7183-7185

ASIAN JOURNAL OF CHEMISTRY

http://dx.doi.org/10.14233/ajchem.2013.14498

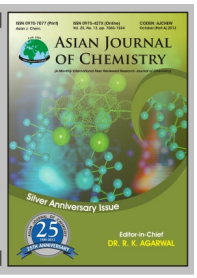

Effects of Calcination Temperature on Properties of Boron Doped TiO_2 Photocatalyst Prepared Using Solvothermal Method

WENJIE ZHANG[1,*], BO YANG[1] and HONGBO HE[2,*]

[1]School of Environmental and Chemical Engineering, Shenyang Ligong University, Shenyang 110159, P.R. China
[2]Institute of Applied Ecology, The Chinese Academy of Sciences, Shenyang 110016, P.R. China

*Corresponding author: Tel: +86 24 83978969; E-mail: metalzhang@yahoo.com.cn; hehongbo@iae.ac.cn

(*Received*: 29 August 2012; *Accepted*: 19 June 2013) AJC-13668

Boron doped TiO_2 based photocatalysts were prepared by solvothermal method at different calcination temperatures. Anatase TiO_2 crystallite sizes of the samples that are calcinated at 300, 400, 500 and 600 ºC are 10.6, 13.3, 19.0 and 28.4 nm, respectively. All the surfaces are rough with small holes and particles distributing on the large particles. The cell volumes of the samples become larger and specific surface areas of the samples decline at higher calcination temperature due to accelerated crystal growth at high temperature. High temperature treatment leads to enlarged average pore size and shrinking pore volume. The sample prepared at 400 ºC shows the optimal photocatalytic degradation activity. Adsorption capacity declines constantly along with increasing calcination temperature.

Key Words: TiO_2, Boron, Photocatalytic, Calcination.

INTRODUCTION

TiO_2 has attracted much attention due to its practical applications such as self cleaning surfaces, wastewater and air purification and bacteria inactivation[1,2]. Most environmental organic pollutants can be degraded by photocatalytic oxidation processes on TiO_2 surface. However, the application of TiO_2 is limited by its large band gap (3.2 eV in the anatase phase) and recombination rate of photogenerated electrons and holes is usually very quickly. Doping technology is one of the effective means to overcome the disadvantages of TiO_2. A variety of nonmetal ions such as N[3,4], C[5], S[6] and B[7] has been explored to promote separation of photogenerated charges in TiO_2. Due to the electron deficiency structure of boron, boron doped TiO_2 has already attracted much attention and researches have increasingly focused on the development of boron doped TiO_2 systems in recent years[8].

In review of the work concerning the properties of photoactive B-TiO_2, most of the work were conducted on effects of B doping amounts. Limited published works were related to the effects of calcination temperature on properties of B doped TiO_2. In the present work, boron doped TiO_2 based photocatalysts were prepared by solvothermal method at different calcination temperatures. Photocatalytic degradation of an organic azo-dye, methyl orange, was investigated under ultraviolet irradiation. The effects of calcination temperature on structure, surface area, crystallinity and photocatalytic activity of B-TiO_2 photocatalyst were investigated.

EXPERIMENTAL

Sol-gel preparation: 3 wt % boron doped TiO_2 photocatalysts were prepared by a modified solvothermal approach. The detailed process was described as follows. Tetrabutyl titanate of chemical pure grade was chosen as the Ti precursor and tributyl borate (99.5 %) was used as the boron source. Hydrochloric acid and anhydrous ethanol were in the analytical reagent grade. The reagents were mixed thoroughly to prepare the precursor in a beaker. Another solution was prepared with anhydrous ethanol and water and then was added dropwise to the former solution under constant magnetic stirring. The final mixed solution was continuously stirred until the formation of a consistent sol. The sol was transferred to a PTFE container in a high pressure stainless reactor. The solvothermal reaction was conducted at 120 ºC for 24 h. After cooling to room temperature, the solid product was separated through filtration and was dried at 80 ºC for 8 h, followed by calcination at temperature described later. The obtained 3 % boron doped TiO_2 was ascribed as 3 % B-TiO_2 in the following experiments.

Characterization: Scanning electron microscope images were taken on a HTACHI S-3400N scanning electron microanalyzer. The samples for SEM imaging were coated with a thin layer of gold film to avoid charging. The crystalline phases of the photocatalysts were measured by X-ray diffraction with D/max-rB diffractometer using a CuK_α radiation. The N_2-adsorption and desorption of the sample was measured by

F-Sorb 3400 specific surface area and pore size distribution analytical instrument. Specific surface areas and pore size distribution were calculated from the N_2 desorption isotherms, according to Brunauer-Emmett-Teller (BET) equation and Barrett-Joyner-Halenda (BJH) method, respectively.

Photocatalytic activity: The photocatalytic activity of B-TiO_2 composite was evaluated by degradation of methyl orange solution under UV light irradiation. The adsorption and photocatalytic activity of the samples were investigated by measuring the decoloration rate of methyl orange in a lab-scale photocatalytic reactor. The reactor consisted of a 250 mL beaker and a UV lamp hanging over the beaker. The 20 W UV-light lamp with main irradiation wavelength at 253.7 nm was used as a light source to trigger the photocatalytic reaction and the average light intensity was about 1100 μW/cm^2. The concentration of methyl orange was calculated by Lambert-Beer law using 721E spectrophotometer. The absorbency of methyl orange was measured at 468 nm corresponding to the maximum absorption wavelength.

The mixed solution of methyl orange and photocatalyst (V = 50 mL, $C_{methyl\ orange}$ = 10 mg/L) was put into a beaker. Before photocatalytic reaction, the adsorption of methyl orange on photocatalyst was measured in the suspension. The solution was allowed to reach an adsorption-desorption equilibrium under 0.5 h of magnetic stirring in the dark. After that, 5 mL of suspension was taken out of the reactor and was filtered through a Millipore filter (pore size 0.45 μm) to remove the catalyst. The filtrated solution was measured for its absorbency. After that, the remaining methyl orange and photocatalyst suspension was put under UV light irradiation. After a distinct time, 5 mL of suspension solution was removed and filtrated to measure the change of methyl orange concentration. If not indicated, the irradiation time in the subsequent experiments was set to 0.5 h.

RESULTS AND DISCUSSION

Fig. 1 shows XRD patterns of 3 % B-TiO_2 samples prepared at different calcination temperature. The diffraction peaks of 3 % B-TiO_2 at (101), (004), (200), (105), (211) and (204) planes are in accordance to those of anatase TiO_2. The diffraction peaks began to appear at calcination temperature of 300 ºC and there is no peaks of other phases of TiO_2. All the samples were doped with 3 % boron and there is no diffraction peaks of any substances containing boron, such as B_2O_3 or TiB_2. This can be explained by the well dispersion of boron in the bulk TiO_2. TiO_2 crystallite formation becomes better at higher calcination temperature. As calculated using Scherrer's formula, anatase TiO_2 crystallite sizes of the samples calcinated at 300, 400, 500 and 600 ºC are 10.6, 13.3, 19.0 and 28.4 nm, respectively.

Surface morphology is essential to properties of photocatalyst. As can be seen in Fig. 2, the samples are calcinated at (a) 300 ºC, (b) 400 ºC, (c) 500 ºC and (d) 600 ºC. All the surfaces are rough, with small holes and particles distributing on the large particles. High temperature calcination results in greater roughness on the surfaces. Grinding of the samples also causes production of the adhered small particles on the large surfaces.

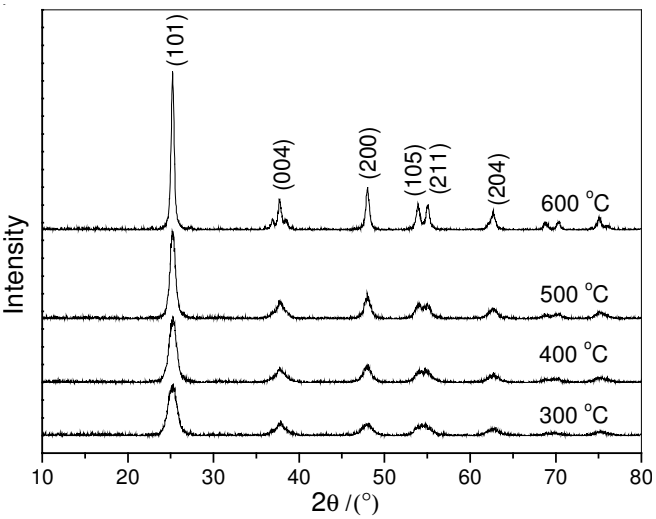

Fig. 1. XRD patterns of 3 % B-TiO_2 samples at different calcination temperature

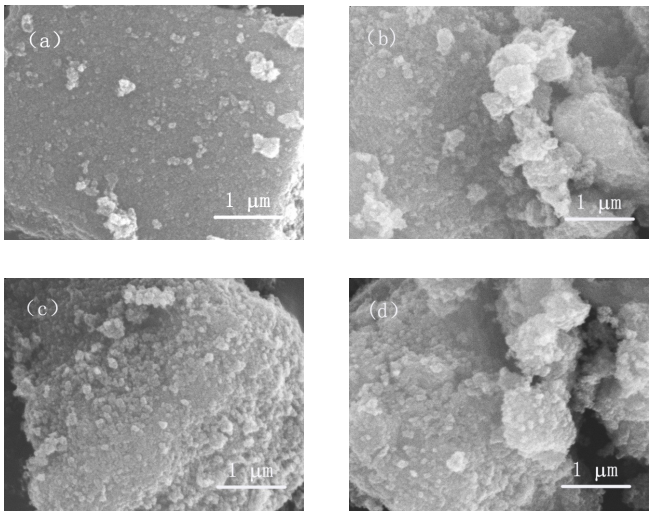

Fig. 2. SEM images of 3 % B-TiO_2 samples calcined at (a) 300 ºC, (b) 400 ºC, (c) 500 ºC and (d) 600 ºC

Lattice parameter and BET surface area of B-TiO_2 samples calcinated at different temperature are listed in Table-1. Specific surface areas of the samples decline at higher calcination temperature because of particles growing and aggregating at high temperature thermal treating. Lattice parameters are obtained by Bragg's law and a formula for a tetragonal system, $1/d^2 = (h^2 + k^2)/a^2 + l^2/c^2$. As summarized in Table-1, the lattice parameters of all the B-TiO_2 samples change along with the change of calcination temperature. The cell volumes of 3 % B-TiO_2 samples become larger at higher calcination temperature due to accelerated crystal growth at high temperature.

TABLE-1
LATTICE PARAMETER AND BET SURFACE AREA OF B-TiO_2 SAMPLES CALCINATED AT DIFFERENT TEMPERATURE

Calcinations temp. (ºC)	Surface area (m^2/g)	a(=b) (10^{-1} nm)	C (10^{-1} nm)	V (10^{-3} nm^3)
300	127.96	3.7780	9.5720	136.624
400	109.56	3.7933	9.5630	137.603
500	70.93	3.8014	9.5438	137.920
600	44.24	3.8025	9.5541	138.141

N_2 desorption isotherm patterns of 3 % B-TiO_2 samples at different calcination temperature is shown in Fig. 3. Calcination temperature has much effect on N_2 adsorption capacity of the samples in an decreasing trend following 300 ºC > 400 ºC > 500 ºC > 600 ºC. The sample calcinated at 300 ºC has the largest N_2 desorption capacity, because organic substances in the sample does not burn out at low temperature treatment.

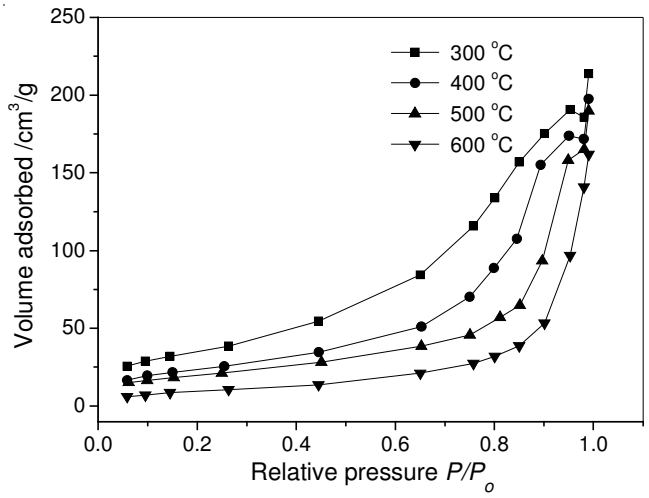

Fig. 3. N_2 desorption isotherm patterns of 3 % B-TiO_2 samples at different calcination temperature

Fig. 4 shows BJH pore size distribution patterns of 3 % B-TiO_2 at different calcination temperature. Pore size of the sample at 300 ºC distributes in the range between 1.5-15 nm, while the distribution range is enlarged when the samples are treated at high temperature. According to the patterns and being calculated using BJH method, the average pore sizes of the samples are 12.2, 16.2, 18.1 and 29.7 nm, alone with increasing calcination temperature. Meanwhile, the total pore volumes of the samples are 0.389, 0.351, 0.321 and 0.277 mL/g, respectively. High temperature treatment leads to enlarged average pore size and shrinking pore volume.

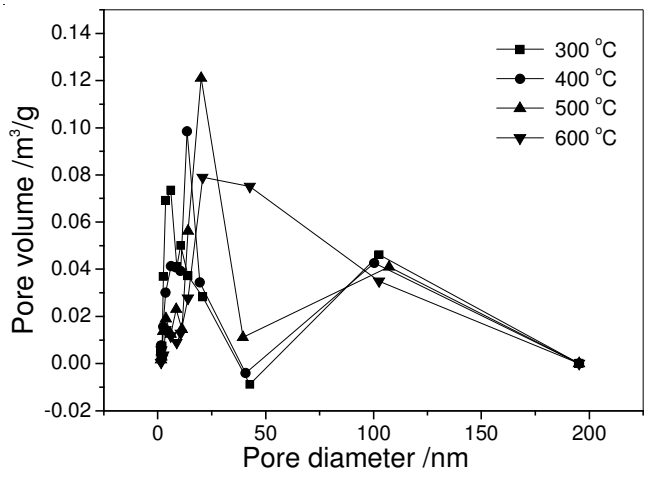

Fig. 4. BJH pore size distribution patterns of 3 % B-TiO_2 at different calcination temperature

Photocatalytic activity and adsorption capacity were also compared for the samples calcinated at different temperature (Fig. 5). It is noticed that adsorption capacity declines

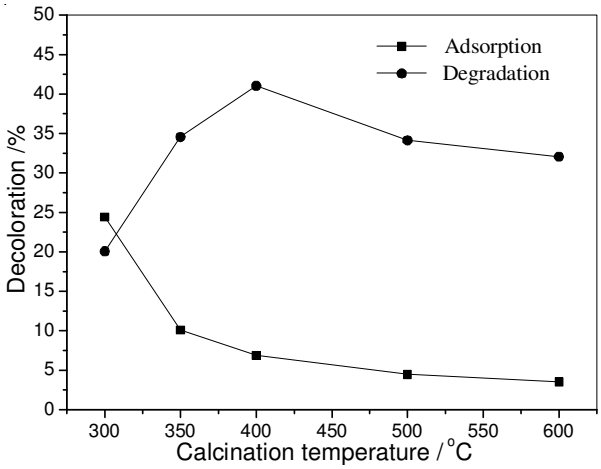

Fig. 5. Photocatalytic activities of 3 % B-TiO_2 samples at different calcination temperature

constantly along with increasing calcination temperature due to the thorough burning out of organic substances in the materials. Photocatalytic activity varies with the change of calcination temperature. The sample prepared at 400 ºC shows the optimal photocatalytic degradation activity which can be attributed to the complex influence of phase transformation and particle growing at different calcination temperature. Anatase TiO_2 possesses the greatest activity as being compared to rutile or amorphous states of TiO_2. Crystalline growing and particle aggregation at high temperature also lead to decreasing photocatalytic activity and adsorption capacity.

Conclusion

The effects of calcination temperature on structure, surface area, crystallinity and photocatalytic activity of B-TiO_2 photocatalyst were investigated. The diffraction peaks of 3 % B-TiO_2 at (101), (004), (200), (105), (211) and (204) planes are in accordance to those of anatase TiO_2. High temperature calcination results in greater roughness on the surfaces. The cell volumes of 3 % B-TiO_2 samples became larger at higher calcination temperature due to accelerated crystal growth at high temperature.

ACKNOWLEDGEMENTS

This work was supported by the National Natural Science Foundation of China (No. 41071161), National Key Basic Research Foundation of China (2011CB403202) and Liaoning Science and Technology Project (2010229002).

REFERENCES

1. G.H. Li, S. Ciston, Z.V. Saponjic, L. Chena, N.M. Dimitrijevic, T. Rajh and K.A. Gray, *J. Catal.*, **253**, 105 (2008).
2. S. Guo, Z.B. Wu, H.Q. Wang and F. Dong, *Catal. Commun.*, **10**, 1766 (2009).
3. M. Qiao, S.S. Wu, Q. Chen and J. Shen, *Mater. Lett.*, **64**, 1398 (2010).
4. J. Senthilnathan and L. Philip, *Chem. Eng. J.*, **172**, 678 (2011).
5. Y. Li, M.Y. Ma, X.H. Wang and X.H. Wang, *J. Environ. Sci.*, **20**, 1527 (2008).
6. H. Tian, J.F. Ma, K. Li and J.J. Li, *Ceram. Int.*, **35**, 1289 (2009).
7. N. Lu, H.M. Zhao, J.Y. Li, X. Quan and S. Chen, *Sep. Purif. Technol.*, **62**, 668 (2008).
8. Y.H. Han, X.L. Ruan, J.Q. Chen, H.M. Zhang, H.J. Zhao and S.Q. Zhang, *Asian J. Chem.*, **25**, 6167 (2013).